Theor Chem Acc (2011) 128:505–519
DOI 10.1007/s00214-010-0831-6

REGULAR ARTICLE

Analysis of the magnetic coupling in nitroxide organic biradicals

Carmen J. Calzado · Celestino Angeli · Coen de Graaf · Rosa Caballol

Received: 30 July 2010 / Accepted: 18 September 2010 / Published online: 7 October 2010

Abstract The magnetic coupling in organic biradicals has been analyzed by means of ab initio wave function-based methods. Attention is focused on the coupling between the spin moments localized on the NO-groups in *meta* and *para* phenylene-bridged nitroxides, and bis(nitronyl) nitroxide and bis(imino) nitroxide biradicals. The leading mechanisms governing the coupling have been isolated by means of class-partitioned CI calculations. It was found that the mechanisms of the coupling in the *para* and *meta* phenylene-bridged nitroxides are similar to that found in transition metal complexes, while for the other biradicals the dominance of other mechanisms (like the spin polarization) imposes restrictions on the computational strategy to be followed to best estimate the coupling.

Published as part of the special issue celebrating theoretical and computational chemistry in Spain.

Electronic supplementary material The online version of this article (doi:10.1007/s00214-010-0831-6) contains supplementary material, which is available to authorized users.

C. J. Calzado (✉)
Departamento de Química Física, Universidad de Sevilla, Professor García González s/n, 41012 Sevilla, Spain
e-mail: calzado@us.es

C. Angeli
Dipartimento di Chimica, Universitá di Ferrara, via Borsari 46, 44100 Ferrara, Italy

C. de Graaf · R. Caballol
Departament de Química Física i Inorgànica, Universitat Rovira i Virgili, Marcel lí Domingo s/n, 43007 Tarragona, Spain

C. de Graaf
Institució Catalana de Recerca i Estudis Avançats (ICREA), Passeig Lluís Companys 23, 08010 Barcelona, Spain

Keywords Magnetic interactions · Organic biradicals · Nitroxide · DDCI, CASPT2 and NEVPT2 calculations · Leading magnetic mechanisms

1 Introduction

Many efforts have been devoted to understand the factors controlling the interactions between the spin moments in magnetic systems. Since the seminal work of Anderson [1, 2], many models have been proposed to explain magnetic exchange interactions. The simplest one-band models only deal with the magnetic orbitals and the unpaired electrons. In these models, the coupling parameter J can be expressed as a function of the direct exchange between the magnetic orbitals, of ferromagnetic character, and the one-electron transfer between magnetic centers and the on-site Coulomb repulsion, both included in the antiferromagnetic (AF) kinetic exchange term also known as the Anderson mechanism of super exchange. A further step adding complexity to the analysis of the physical effects is made in two-band models [3], which include orbitals located on the diamagnetic bridges between magnetic centers to take explicitly into account the bridge to magnetic center charge transfer mediating the coupling between the neutral and ionic determinants in a valence bond (VB) description [4]. Both types of analysis have essentially concerned systems with metallic magnetic centers.

At the same time, ab initio calculations have been able to provide accurate values of the coupling parameter in systems of increasing complexity and size. Both density functional theory (DFT) and wave function-based methods have extensively been used and their performances and limitations are discussed at length in the literature [5–9]. These calculations have also helped to clarify some aspects

of the factors governing the coupling. In particular wave function-based calculations have put in evidence that the J values resulting from the action of the exact Hamiltonian on the model space associated to one-band and two-band models are at least one order of magnitude smaller than experiment or even of incorrect sign, making evident more complex coupling mechanisms.

In a pioneering work in the early 80s, de Loth et al. [10–12] analyzed the physical contributions to the magnetic coupling beyond the active-electron only approximation. Following an idea developed by Malrieu [13], they provided expressions for the perturbation theory (PT) evaluation of J from the energy gap between the singlet and triplet states of dinuclear Cu (II) complexes. Inspired by this work, Broer and Maaskant performed variational calculations including the same configurations on copper dinuclear complexes [14]. The further developments of these ideas led to the formulation of the Difference Dedicated Configuration Interaction approach (DDCI) [15, 16], where the CI expansion only contains the configurations that play a role in the energy difference of the states involved in the coupling. Recent developments as the Spectroscopy Oriented CI (SORCI) method, developed by Neese [17, 18], and the modified DDCI2 method of Barone et al. [19] are based on the same arguments. The DDCI approach has been extensively employed in the evaluation of magnetic properties in molecular [20–33] and solid-state magnetic materials [34–39], with a remarkable good agreement with experiment.

Alternatively, one can approach the magnetic properties within the framework of the density functional theory. Most often the description of the antiferromagnetically coupled state relies on the broken symmetry approach [40–47], although several alternatives have been reported in the literature [48–53]. Another point of interest is how to choose the most appropriate functional in the calculations. The B3LYP functional has been widely applied and many important contributions have been made to the field of molecular magnetism [54–56]. Recent developments in the derivations of new functionals led to a series of papers in which the performance of the different functionals is tested [57–64]. In addition to this rather methodological work, there is an overwhelming amount of articles in which DFT-based methods are applied to molecular complexes and solid-state compounds, see Refs. [65, 66] for two recent reviews.

DDCI has been used to analyze in depth the physical contributions to the magnetic coupling on a series of dinuclear Cu (II) complexes by partitioning the CI space in different classes of contributions [67, 68]. After classifying the excitations according to the number of doubly occupied orbitals (h) and virtual orbitals (p) implied in the excitation that acts on the determinants of the reference wave function, the results have shown that two main classes of excitations are determinant in the coupling: (1) The $1h$-$1p$ class of excitations involving one inactive occupied orbital h and one inactive virtual orbital p introduce spin polarization effects as well as the polarization of the ionic forms. Both effects are particularly important when they involve orbitals centered in the bridging ligands; (2) The $2h$-$1p$ and $1h$-$2p$ classes of excitations, representing single excitations on the ligand-to-metal charge transfer (*LMCT*) and metal-to-ligand charge transfer (*MLCT*) configurations, respectively. As discussed recently [68], the crucial role of these two types of excitations must be attributed to higher order effects (*interactions between excited configurations*), leading in AF systems to an increase in the weight of the *LMCT* configurations. This increase can be interpreted as a correlation-induced delocalization of the magnetic orbitals on the ligands. This causes the magnetic orbitals to take larger tails on the bridging ligands and therefore both direct exchange and kinetic exchange increase.

Until now, our analysis of the different contributions to the magnetic coupling has basically been concerned with systems including metallic magnetic centers bridged by diamagnetic ligands, leaving aside the organic magnetic systems. Given the importance of these systems in technologically potentially interesting systems, we present here the analysis of the magnetic coupling in some non-metallic biradicals. We focus on two well-studied examples: phenylene-bridged nitroxide biradicals and Ullman's bis(nitronyl) and bis(imino) nitroxides. A brief recall of the main results of this type of analysis in bimetallic systems is given in Sect. 2. Sections 3 and 4 describe the systems objects of this analysis and the corresponding computational details. The results are discussed in Sect. 5 and the main conclusions summarized in Sect. 6.

2 Recall of relevant mechanisms in the magnetic coupling of S = ½ metallic dinuclear systems

The interaction between the unpaired electrons located on different sites can be interpreted as an effective interaction between site-centered spins and mapped onto the Heisenberg-Dirac-Van Vleck Hamiltonian: [69–71]

$$\hat{H} = -\sum_{i,j} J_{ij} \hat{S}_i \cdot \hat{S}_j \tag{1}$$

where J_{ij} is the nearest neighbor coupling parameter, and $\hat{S}_i$ is the total spin operator on site i. For systems with two magnetic sites, Eq. 1 reduces to

$$\hat{H} = -J\, \hat{S}_1 \cdot \hat{S}_2 \tag{2}$$

and the energy spectrum given by the Heisenberg Hamiltonian is directly related with the coupling parameter through the Landé rule, which gives the separation between two spin states of total spins S and $S-1$:

$$E(S) - E(S-1) = -JS \tag{3}$$

In particular, for S = ½ dinuclear systems, the coupling parameter is given by the separation between the triplet and the singlet states:

$$^1E - {}^3E = J \tag{4}$$

In this formulation, the ferromagnetic behavior associated with a triplet ground state gives a positive J. According to the Anderson mechanism, the coupling parameter results from two antagonist contributions:

$$J = J_{\mathrm{F}} + J_{\mathrm{AF}} \tag{5}$$

where the ferromagnetic contribution (F) is attributed to the direct exchange between spin moments, while the AF counterpart is originated by delocalization effects and its analysis reaches different levels of complexity depending on the model used.

The valence models deal only with magnetic orbitals and the unpaired electrons (one-band model) or include one or a few ligand orbitals (two-band model). In systems with two S = ½ sites, the one-band model reduces to two electrons in two magnetic orbitals a and b, giving two neutral determinants, $N = \{|a\bar{b}|, |b\bar{a}|\}$, with one electron per site and two ionic determinants, $I = \{|a\bar{a}|, |b\bar{b}|\}$, with the two electrons in the same site (for simplicity, the core orbitals have been omitted in the notation). These four determinants define a minimal valence Complete Active Space (CAS), a CAS(2,2). In an orthogonal context, the localized magnetic orbitals can simply be obtained by rotation of the symmetry-adapted CASSCF active orbitals. From second-order perturbation theory or from the CAS CI matrix representation [67], it can be demonstrated that Eq. 4 gives an expression for J that depends on three parameters:

$$J = 2K_{ab} - \frac{4t_{ab}^2}{U} \tag{6}$$

The first term, also called direct exchange, is twice the exchange integral between the magnetic orbitals a and b, $K_{ab} = \langle a\bar{b}|\hat{H}|b\bar{a}\rangle$, and is ferromagnetic; the second term, the kinetic exchange, depends on the one-electron transfer between metal centers $t_{ab} = \langle a\bar{b}|\hat{H}|a\bar{a}\rangle$ and the relative energy of the ionic determinants with respect to the neutral ones or on-site Coulomb repulsion U. This contribution driven by the coupling between neutral and ionic VB configurations takes into account the delocalization effects and is antiferromagnetic.

To take into account the role of the ligands in the magnetic coupling mechanisms in systems with metallic magnetic centers, two-band models have been derived that include orbitals located on diamagnetic bridging ligands. The ligand-to-metal charge transfer (*LMCT*) contributions

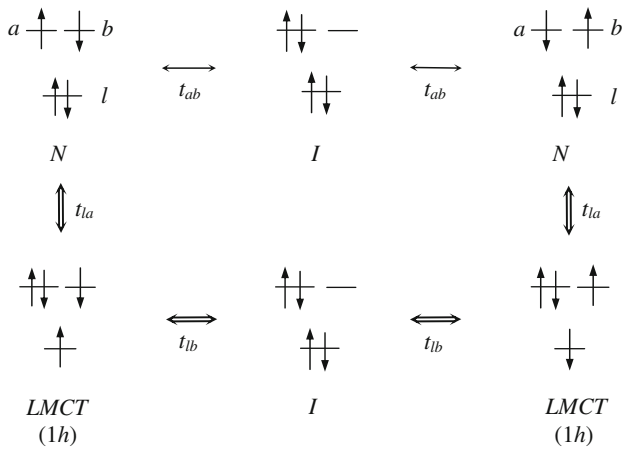

Fig. 1 Schematic representation of one-band (*left right arrow*) and two-bands (*left right double arrow*) mechanisms in S = ½ dinuclear systems

mediate the coupling between the neutral and ionic VB determinants and modify the electron transfer integral:

$$J = 2K_{ab} - \frac{4\left(t_{ab}^{eff}\right)^2}{U} \tag{7}$$

In its simplest version, only one ligand orbital is added (l) and the resulting model includes four electrons in three orbitals for S = ½ dinuclear systems. The main effect of *LMCT* configurations is to add second-order corrections to the hopping integral t_{ab} (i.e. fourth-order corrections to J) through the mechanism depicted in Fig. 1, thus enhancing the antiferromagnetic character:

$$t_{ab}^{eff} = t_{ab} + \frac{t_{al}t_{bl}}{\Delta E_{CT}} \tag{8}$$

The correction is expressed in terms of the one-electron hopping integral between metal and ligand orbitals, t_{al} or t_{bl}, and the ligand-to-metal charge transfer excitation energy ΔE_{CT}. Other mechanisms can be invoked, implying double *LMCT* configurations, but are supposed to play a minor role due to the high relative energy of these configurations.

As discussed previously [67, 68], the use of an optimized set of molecular orbitals makes that the formal distinction between one- and two-band models looses its significance. The variational optimization induces an important mixing of ligand and magnetic orbitals, and furthermore, the ligand–metal hopping integrals become null due to Brillouin's theorem [72, 73]. Numerical results at the valence level have shown that the J values obtained including only the valence effects are in general far from the experimental value [67, 68] and that important contributions arise from dynamic electron correlation.

The excitation processes upon CAS configurations can be classified in terms of the inactive doubly occupied

(h) and virtual orbitals (p) implied in the excitation. The analysis of their role in S = ½ dinuclear systems has shown that three classes of excitations have a relevant role in the coupling:

a. The excitations involving one inactive occupied and one virtual orbital, the 1h-1p class of excitations, that can preserve or not the singlet character of the inactive part.

   (a1) The main effect of the processes preserving the spin of the inactive part, $\hat{a}_p^\dagger \hat{a}_h$ or $\hat{a}_{\bar{p}}^\dagger \hat{a}_{\bar{h}}$ on the CAS determinants, $\left(\hat{a}_p^\dagger \hat{a}_h + \hat{a}_{\bar{p}}^\dagger \hat{a}_{\bar{h}}\right)$ in case of configuration state functions) is the polarization of the ionic VB forms, and their contribution consists in lowering the effective energy of these ionic configurations, U_{eff}. They only contribute to the singlet state and therefore enhance the AF component of the coupling constant.
   (a2) Among the 1h-1p class, the excitation processes that do not preserve the spin of both the active and the inactive parts, $\hat{a}_p^\dagger \hat{a}_{\bar{h}}$ or $\hat{a}_{\bar{p}}^\dagger \hat{a}_h$ on the neutral VB determinants, $|a\bar{b}|, |b\bar{a}|$ (shown in Scheme 1) induce spin polarization effects, which contribute both to the singlet and to the triplet states, and their global effect can be F or AF.
   Both types of contributions are particularly important when they involve orbitals centered on the bridging ligands, as shown in early second-order estimations and in variational calculations [10–12, 67, 68].

b. The excitations involving two inactive occupied and one virtual orbitals, the 2h-1p class. Different pathways of interaction have been proposed that favor either AF or F effects. The interaction pathways appear at higher than second-order perturbation theory, and their magnitude can only be addressed in variational calculations due to the important synergy with other classes of excitations.

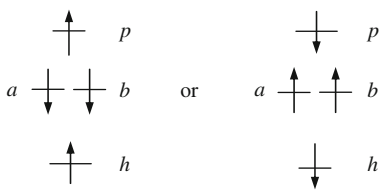

Scheme 1 1h-1p determinants causing spin polarization effects

   (b1) The first pathway stabilizes the ionic configuration through the coupling with *both* the 1h and 1h-1p excitations, and introduces an AF effect:

   $N \leftrightarrow I \leftrightarrow LMCT(1h) \leftrightarrow 2h\text{-}1p \leftrightarrow N$

   (b2) The second one is not mediated by ionic configurations, as for instance:

   $N \leftrightarrow 2h\text{-}1p \leftrightarrow LMCT(1h) \leftrightarrow 2h\text{-}1p \leftrightarrow N$

   and appears to be relevant in ferromagnetic systems.

   Both pathways are present simultaneously, playing in favor of AF or F contribution, which become dominant depending on the nature of the system under study.

c. The excitations involving one inactive occupied and two virtual orbitals, the 1h-2p class, play a non-negligible damping role of the precedent class, balancing the AF systems with an F contribution, and with a small AF effect for the F systems. Although a dominant pathway has not been proposed, their effect is due to high order interferences with the 2h-1p class.

3 Description of the systems

Nitroxides have attracted considerable attention due to the stability of different radicals or polyradicals in this family that make them suitable building blocks to be combined with different couplers to give extended molecular magnetic architectures. Phenylene is one of these groups, acting as an AF coupler when substituted in *para*, but as a robust F coupler when substituted in *meta*. On the other hand, there is a wide family of compounds based on nitronyl-nitroxide radical bridged by a large variety of groups, among which are conjugated and aromatic bridges. We analyse here the simplest members of these two families shown in Scheme 2, namely *meta* and *para* phenylene dinitroxides (a and b, respectively) and a bis(nitronyl)nitroxide and its bis(imino) analog (c and d, respectively) based on Ullman biradicals [74], where methyl substituents have been replaced by hydrogen.

Concerning the phenylene-bridged models (a) and (b), the *meta* isomer (a) as well as some substituted derivatives have been the object of considerable theoretical attention, in order to interpret the experimental discrepancy from the well-known F behavior of the bridging group found in some substituted *meta* phenylene-bridged dinitroxides exhibiting AF behavior [75, 76]. Fang et al. [77] have rationalized from GVB and ROHF calculations that the anomalous AF behavior is due to the loose of planarity and

Scheme 2 Representations of meta (**a**) and para (**b**) phenylene dinitroxide, and bis(nitronyl) nitroxide (**c**) and bis(imino) analoge (**d**)

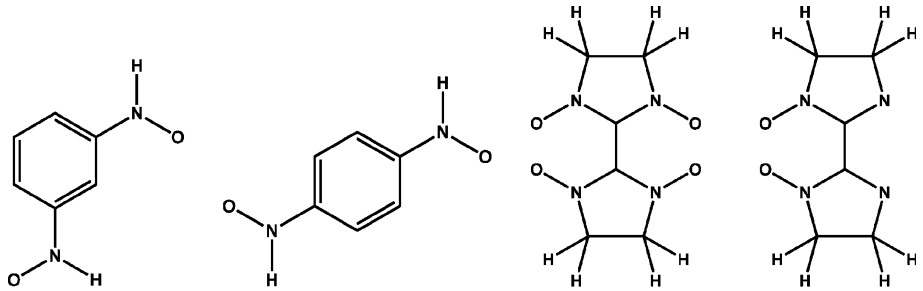

(a) **(b)** **(c)** **(d)**

estimated the triplet state, both for the planar *syn* (represented in model (a)) and *anti*-isomers, to be 0.28 kcal/mol more stable, i.e. 98 cm^{-1}. Semi-empirical calculations oriented to qualitatively explain the magnetic behavior in front of substituents have also been performed [78]. B3LYP calculations by Mitani et al. [79], in the framework of a systematic study on the functional and substituents dependence, and Catala et al. [80] give ferromagnetic estimates of singlet–triplet gap for the planar model of 462 and 428 cm^{-1}, respectively. Both *meta* (a) and *para* isomers (b) have also been the object of extensive attention of Barone and collaborators, both with DFT calculations [81] and multireference CI level in a series of papers essentially oriented to define efficient wave function-based strategies [19, 81, 82]. The singlet–triplet gaps found for the *meta* and *para* isomers with a 6-31G(d) basis set are 568 and $-1{,}861$ cm^{-1} with DDCI2 and 371 and $-1{,}807$ cm^{-1} with DDCI, whereas B3LYP calculations with the same basis set gives 561 and $-2{,}100$ cm^{-1} [83]. Experimentally, the singlet–triplet gap of *meta* phenylenebis(*tert*-butyl nitroxide) biradical was estimated to be 695 cm^{-1} [84].

Alies et al. have determined the X-ray structure of Ullman's nitroxides as well as their magnetic characterization [85]. The crystal structure shows that both nitroxides are twisted by an angle of 54°–55°, although bis(imino)nitroxide exhibits a statistical disorder involving the oxygen atom of the NO groups, due to the presence of several isomers in the crystal. Magnetic susceptibility measurements, both in the solid state and in solution, have shown antiferromagnetic behavior of both compounds with coupling constants in the solid phases of -311 and -194 cm^{-1}, for bis(nitronyl)nitroxide and bis(imino)nitroxide, respectively.

Ullman's type biradicals have been the object of several theoretical studies, both at the multireference CI level [19, 86] and within DFT approaches [87, 88]. The calculated J values at DDCI2 level give similar values around -360 cm^{-1} for model (c) [19, 86]. B3LYP results by Ali and Datta [87] on the whole Ullman's bis(nitroxyl)nitroxide coupling parameter range from -277 to -281 cm^{-1} depending on the basis set, although in view of the definition of the Heisenberg Hamiltonian given in the paper, the estimated singlet–triplet gap seems to be twice this value, giving therefore a strong overestimation in relation to experiment (at difference to the present definition, which gives the coupling parameter from Eq. 4). Model (d) of Ullman's bis(iminino)nitroxide has as well been studied with several DFT approaches [88] with results ranging from -122 to -214 cm^{-1} depending on the functional.

4 Computational information

The exact (non-relativistic) wave functions and energy eigenvalues of the different electronic states involved in the magnetic coupling are approximated by a variety of computational methods that can be classified into two major groups. In the first place, the variational methods like the complete active space + singles (CAS + S), and difference dedicated configuration interaction (DDCI or DDCI2). On the other hand, we also apply approaches based on perturbation theory as complete active space second-order perturbation theory (CASPT2) [89–91] and *n*-electron valence state second-order perturbation theory (NEVPT2) [92–95]. The reader is referred to the original papers for a detailed description of these methods; here, we only recall the most essential points.

Both the perturbative and variational methods take a multiconfigurational reference wave function that is obtained as a complete active space self-consistent field (CASSCF) wave function with either a minimal active space of two electron and two orbitals or an extended active space with six electrons and six orbitals. The character of the active orbitals is specified for each system in the discussion of the results. In CASPT2 and NEVPT2 state specific orbitals have been used, while the DDCI calculation needs a common set of orbitals for both the singlet- and triplet-coupled states. Here, we follow the common practice to express both states in the molecular orbitals resulting from a CASSCF calculation on the triplet state. Other choices for a common orbital set (for instance

singlet–triplet averaged orbitals) only weakly affect the final estimates of the coupling parameter.

The CI matrix of the DDCI calculations is spanned by a well-defined subset of determinants generated by all single and double replacements from the determinants of the CAS. A quasi-degenerate second-order perturbation analysis [16] shows that the double replacements involving only inactive and virtual orbitals cause a uniform shift of the diagonal matrix elements. Hence, on the basis of these perturbation arguments, these determinants can be eliminated from the CI expansion without consequences for energy differences of the states of interest. The CAS + S and DDCI2 variants of the full DDCI scheme further reduce the CI expansion as shown in Fig. 2. Class-partitioned CI spaces are obtained by adding to the valence CAS selected classes of excited configurations belonging to DDCI. In summary, full DDCI includes all single and double excitations on top of the defined CAS, with the exception of purely "inactive" ones that excite two electrons of the inactive doubly occupied orbitals into the virtuals. As DDCI, all the class-partitioned CI calculations are uncontracted calculations and all give eigenfunctions of the total spin $\hat{S}^2$ operator by imposing the required symmetry relations between the corresponding determinants.

CASPT2 and NEVPT2 estimate the effect of electron correlation on the energy with second-order perturbation theory. While the CASPT2 zeroth-order Hamiltonian is based on an effective one-electron Fock-type operator, NEVPT2 uses the Dyall Hamiltonian [96] to define the zeroth-order that is a Hamiltonian with two-electron interactions. An important advantage of NEVPT2 in comparison with CASPT2 is the absence of intruder states in the former one. The two methods use a contracted reference wave function, but NEVPT2 offers also different levels of contraction in the first-order interacting space

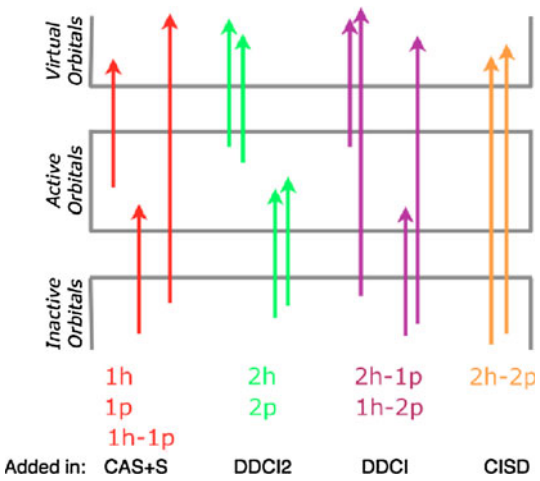

Fig. 2 Subdivision of the single and double replacements out of the CAS reference wave function for CAS + S, DDCI2, and DDCI

(FOIS). Here, we use the partially contracted implementation of NEVPT2, in which the FOIS is the same as used in CASPT2. Both schemes have been applied to the calculation of the coupling between paramagnetic transition metal (TM) centers in complexes. In general, standard NEVPT2 systematically underestimates the coupling by approximately 40%. Similar observations were made for CASPT2, while this method becomes numerically unstable for coupling parameters smaller than ~ 20 cm^{-1} [32].

The one-electron basis set used in the calculations is of atomic natural orbitals type [97]. For C, N, and O, a basis set with (3s,2p,1d) contracted function was applied, while a (2s) basis set was centered on the H atoms. Test CASPT2 calculations with larger basis sets (4s,3p,2d and 3s,1p) result in magnetic coupling parameters that are less than 5 cm^{-1} different than those obtained from the smaller basis set. The dynamic electron correlation was taken into account for all electrons, except the electrons in the 1s orbitals of the C, N, and O atoms. The IPEA shift in the CASPT2 zeroth-order Hamiltonian [98] was put to zero, since this choice leads to numerically more stable magnetic coupling parameters as shown previously [32]. CASSCF and CASPT2 calculations were performed with the MOLCAS 7 code [99], DDCI calculations with the CASDI set of programs [100] and the NEVPT2 calculations were performed with a computational package developed at the University of Ferrara.

We have used the experimental structure for bis(nitroxyl)nitroxide [85] in the calculations. The geometries of the other systems are either not available (phenylene-bridged systems) or show disorder (bis(imino) nitroxide). Therefore, the geometry of these molecules have been optimized with CASPT2 using the triplet CAS(2,2) wave function as reference. Geometries optimized for the singlet state are practically identical. In the case of bis(imino)nitroxide, we fixed the N–C–C–O dihedral angles to the experimental values. The CASPT2 geometry of the phenylene systems is close to the B3LYP geometries reported in Ref. [81]. The cartesian coordinates of the geometries employed in our calculations are provided in the Supporting Information.

5 Results and discussion

5.1 Phenylene-bridged nitroxide biradicals

Table 1 collects the results obtained for *para* and *meta* bis-nitroxide species from different theoretical approaches. The correlation included in the different CI approaches is shown in Fig. 2. Both systems present remarkable magnetic coupling constants, the nature of the interaction being in agreement with Ovchinnikov's rule: antiferromagnetic

Table 1 Magnetic coupling constant (cm^{-1}) for phenylene-bridged nitroxide biradicals obtained from different approaches

	Para	Meta
CASSCF(2,2)	−765	150
CASPT2	−2,912	705
NEVPT2	−2,732	677
CAS + S	−1,902	698
DDCI2	−2,109	658
DDCI	−1,967	421
DDCI2 6-311 + G(d,p) [81]	−1,942	553
DDCI2 6-31G(d) [83]	−1,861	568
DDCI 6-31G(d) [83]	−1,807	371
UB3LYP 6-311 + G(d,p) [81]	−2,165	655
Experiment [84]	–	695

The reference wave function in all DDCI calculations is a CAS(2,2)CI wave function expressed in the MOs optimized for the triplet state. Experimental data on tert-butyl substituted nitroxide

for the *para* biradical and ferromagnetic for the *meta* compound [101]. The sign of J is well reproduced at the CASSCF level, but the out-of-CAS correlation effects are not negligible at all, as expected. When correlation is taken into account, the absolute J value increases by a factor of ~3 at DDCI level and ~4 in the case of multiconfigurational second-order perturbative approaches. Extending the active space with the π orbitals of the phenylene bridge increases the perturbative estimates of J in a significant way. CASPT2 based on this extended CAS(8,8) gives −3,978 and 1,758 cm^{-1} for the *para* and *meta* compounds, respectively. NEVPT2 shows a similar behavior, although the increase is slightly smaller for the *para* compound. The results based on the extended CAS are −3,276 and 1,787 cm^{-1} for *para* and *meta*, respectively. Hence, it should be stressed that the uncertainty in the perturbative estimates is large and should be taken with caution.

The largest impact on the J values of the dynamic electron correlation is obtained at the CAS + S level. The corresponding CI space is spanned by all the single excitations on top of the CAS(2,2) reference space. As explained in Sect. 2, a particularly important group is formed by the $1h$-$1p$ excitations, which are responsible for the spin polarization effects and the polarization of the ionic forms. While the sign of the former is difficult to predict, the latter stabilizes the ionic forms and favor the singlet state. Consequently, the polarization of the ionic forms increases the absolute value of the AF magnetic coupling. This point will be discussed below in detail. When the CI space is enlarged with $2h$ and $2p$ excitations (DDCI2 space), only a minor effect is observed on the J values, in agreement with previous analysis on bimetallic magnetic systems [67].

Less usual is the impact of the excitations of the DDCI space. Unlike dinuclear transition metal complexes, the inclusion of the $2h$-$1p$ and $1h$-$2p$ excitations lead to a decrease in J with respect to the values obtained at DDCI2 level, i.e. a ferromagnetic effect for the *para* derivate and an AF effect for the *meta* compound. Similar behavior has been obtained by Barone et al., see Table 1 [81, 83]. This observation deserves a deeper analysis, which can be performed by means of the class-partitioned CI, that is, diagonalizing different CI matrices containing only certain types of excitations [68]. This allows us to isolate the individual effects of each type of excitations contained in the DDCI space. The results obtained for these systems using this tool are reported in Table 2 and can be summarized as follows.

Regarding the excitations of the CAS + S space, $1h$ and $1p$ classes have a negligible effect on the magnetic coupling, due to Brillouin theorem [72, 73] as previously discussed in Refs. [67] and [68]. The main contribution comes from the $1h$-$1p$ excitations (see CAS + $1h$-$1p$ entry in Table 2), especially for *meta* compound. As mentioned earlier, this subset contains two types of excitations: those responsible for the polarization of the ionic forms and those carrying the spin polarization (SP) effects. It is possible to isolate most of the SP effects by selecting all the out-of-CAS triplet $\pi \rightarrow \pi^*$ excitations, obtained by applying $\hat{a}^{\dagger}_{\pi^*}\hat{a}_{\bar{\pi}}$ and $\hat{a}^{\dagger}_{\bar{\pi}^*}\hat{a}_{\pi}$ on $N = \{|a\bar{b}|, |b\bar{a}|\}$ references, as exemplified in Scheme 3.

The J values obtained with this subset (CAS + SP entry in Table 2) indicate that this effect is AF for the *para* compound, representing around 45% of the CAS + S J value, while it is the dominant F effect in the *meta* compound. In fact, the coupling of the CAS with the SP configurations gives around 84% of the CAS + S J value. The remaining effect comes from $1h$-$1p$ excitations that

Table 2 Class-partitioned CI estimates of J (cm^{-1}) for phenylene-bridged nitroxides using the CAS(2,2) triplet state MOs and minimal active space

	Para	Meta
CASCI	−540	169
CAS + S	−1,901	698
DDCI2	−2,108	658
DDCI	−1,966	421
CAS + $1h$	−580	158
CAS + $1p$	−670	163
CAS + $1h$-$1p$	−1,064	509
CAS + SP	−863	586
CAS + $1h$ + $2h$-$1p$	−858	**430**
CAS + $1h$-$1p$ + $2h$-$1p$	−979	266
CAS + S + $2h$-$1p$	**−2,247**	700
DDCI2 + $2h$-$1p$	−2,447	629
DDCI2 + $1h$-$2p$	−1,723	439

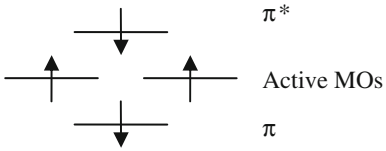

Scheme 3 Triplet $\pi \rightarrow \pi^*$ excitation causing the main spin polarization effect

preserve the spin of the inactive part and produce the polarization of the ionic forms. Figure 3 shows the active MOs for the *para* biradical as well as the occupied π and virtual π^* MOs involved in the dominant SP excitation on the ground state CAS + S wave function. The corresponding MOs of the *meta* species present similar shapes. The key role of spin polarization on magnetic interactions has been extensively invoked by Yamaguchi et al. in the past, regarding the intermolecular through-space interactions in organic radicals [102, 103]. Regarding intramolecular interactions, Barone and co-workers discussed the importance of the SP effects on the relative stability of the singlet and triplet states on *para* and *meta* based on the analysis of the spin population of the C atoms of the aromatic ring [83]. Here, we numerically corroborate the impact of the SP effect on the *J* values in both systems.

When the DDCI2 space is extended with the 2*h*-1*p* and 1*h*-2*p* configurations, i.e. the full DDCI space is considered, the magnetic coupling diminishes in absolute value. This is the result of two opposite effects involving the 2*h*-1*p* and 1*h*-2*p* excitations. The 2*h*-1*p* excitations govern mainly two mechanisms: (1) the stabilization of the ionic forms, through the coupling with *both* the 1*h* and 1*h*-1*p* excitations, which favors the singlet state, and hence, introduces an AF effect and (2) a ferromagnetic pathway coupling the neutral forms, which also involves the 1*h* excitations. For AF systems, where the singlet state wave function has a non-negligible contribution of the ionic configurations, the former mechanism is the

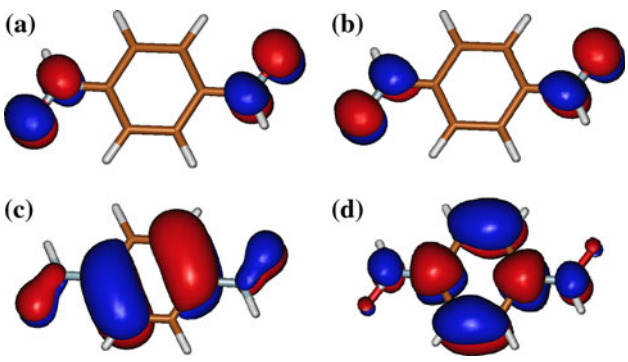

Fig. 3 Active orbitals for *para* phenylene nitroxide (**a**, **b**) and occupied π and virtual π^* MOs involved in the dominant SP excitation (**c**, **d**)

Table 3 Ionic/neutral coefficients ratio on the singlet wave function for phenylene-bridged nitroxides obtained from minimal CAS DDCI calculations

	Para	Meta
CASCI	0.0800	0.0016
CAS + S	0.1657	0.0002
DDCI2	0.1887	0.0009
DDCI	0.1871	0.0026

dominant, and the 2*h*-1*p* excitations give a net AF effect, while for F systems, where the singlet state is essentially represented by the neutral forms, the second pathway dominates the interaction, then producing an F effect.

The *para* and *meta* biradicals belong to these different scenarios as can be seen in Table 3, which contains the ratio of the ionic/neutral configurations on the singlet state for these systems. This ratio is obtained from the projection of the CI wave functions on the CAS space taking into account the composition of the symmetry-adapted active orbitals. As can be seen in Fig. 3, the active orbitals of the *para* compound (and similar for the *meta* biradical) correspond to the symmetric and antisymmetric combination of the π- NO orbitals. Then each active site (*a* or *b*) is not atomic but involves the NO group, and consequently, the ionic forms correspond to those with two electrons in the same nitroxide group of the molecule (left-left or right-right charge localization).

In fact, a large AF effect is observed for the *para* system when the DDCI2 space is enlarged with the 2*h*-1*p* excitations (DDCI2 + 2*h*-1*p* entry in Table 2). The weight of the ionic forms increases significantly in the DDCI wave function compared to the CASCI wave function, which means that the ionic forms are stabilized by the out-of-CAS correlation effects. To illustrate that this AF pathway involving 2*h*-1*p* needs the cooperative effect of both 1*h* and 1*h*-1*p* excitations, three separate calculations have been performed: CAS + 1*h* + 2*h*-1*p*, CAS + 1*h*-1*p* + 2*h*-1*p*, and CAS + S + 2*h*-1*p* (the latter contains both 1*h* and 1*h*-1*p*). The *J* values obtained in these three different CI are −858, −979, and −2,247 cm^{-1}, the last being slightly overestimated with respect to the DDCI value. The same set of calculations for *meta* system gives $J = 482$, 266, and 700 cm^{-1}. In this case, the 2*h*-1*p* excitations introduce a net ferromagnetic contribution, as expected for a system with a negligible weight of the ionic forms (Table 3). Particularly interesting is the *J* value obtained at CAS + S + 2*h*-1*p* level, larger than the two other ones and again overestimated with respect to the DDCI value. This could suggest the presence of a cooperative effect between 1*h* and 1*h*-1*p* excitations also in the ferromagnetic pathway. This has not been observed for dinuclear transition metal complexes up to now, probably because in such

systems the 1*h*-1*p* excitations are too high in energy with respect to the configurations of the CAS. However, in organic biradical systems, the conjugated π framework provides a set of occupied and virtual MOs close in energy to the orbitals in the CAS, which produces 1*h*-1*p* excitations of much lower energy than in TM compounds, and hence, with a larger impact on this mechanism. This effect requires additional tests prior to be considered as a universal behavior in organic biradical systems.

As previously observed, the 1*h*-2*p* class of excitations produce a damping of the global 2*h*-1*p* effect, in such a way that they introduce a ferromagnetic contribution in AF systems and antiferromagnetic in F systems. This effect is evidenced by comparing DDCI with DDCI2 + 2*h*-1*p* results in Table 2.

In summary, the final DDCI estimate of *J* is the result of the competition between several pathways, playing in favor of AF or F contributions. The prevalence of a particular mechanism depends on the weight of the ionic configurations and/or the relative energy of intermediate configurations. Despite the complexity, it has been possible to isolate the leading mechanism of the magnetic coupling between the NO groups in *para* and *meta* phenylene-bridged nitroxide biradicals taking benefit of the class-partitioned CI tool. The excitation classes introducing the largest effects are highlighted in Table 2, and as discussed earlier, they are essentially equivalent to those observed for dinuclear transition metal complexes.

5.2 Ullman's biradicals

The structural and magnetic properties of bis(nitronyl) nitroxide and bis(imino) nitroxide biradicals have been reported by Alies et al. [85]. Magnetic susceptibility measurements show an antiferromagnetic behavior in both compounds, the singlet–triplet gaps being estimated as -311 and -194 cm^{-1}, respectively. The *J* value for bis(imino) nitroxide radical has to be taken with caution, since one of the two independent molecules in the asymmetric unit exhibits a statistical disorder involving the oxygen atom of the NO groups. Several conformers corresponding to the relative positions of the NO groups in the disordered molecule are present, and then the reported *J* value refers to an average of all the interactions corresponding to the different conformers [85].

We start by calculating the singlet–triplet gaps by means of second-order perturbative approaches and DDCI calculations on the basis of a two electrons/two orbitals CAS (Fig. 4c and d). The *J* values obtained for these two systems with minimal CAS and different approaches are reported in Table 4. A large dispersion is observed between perturbative and variational values. In particular CASPT2 and NEVPT2 values are overestimated, while DDCI values

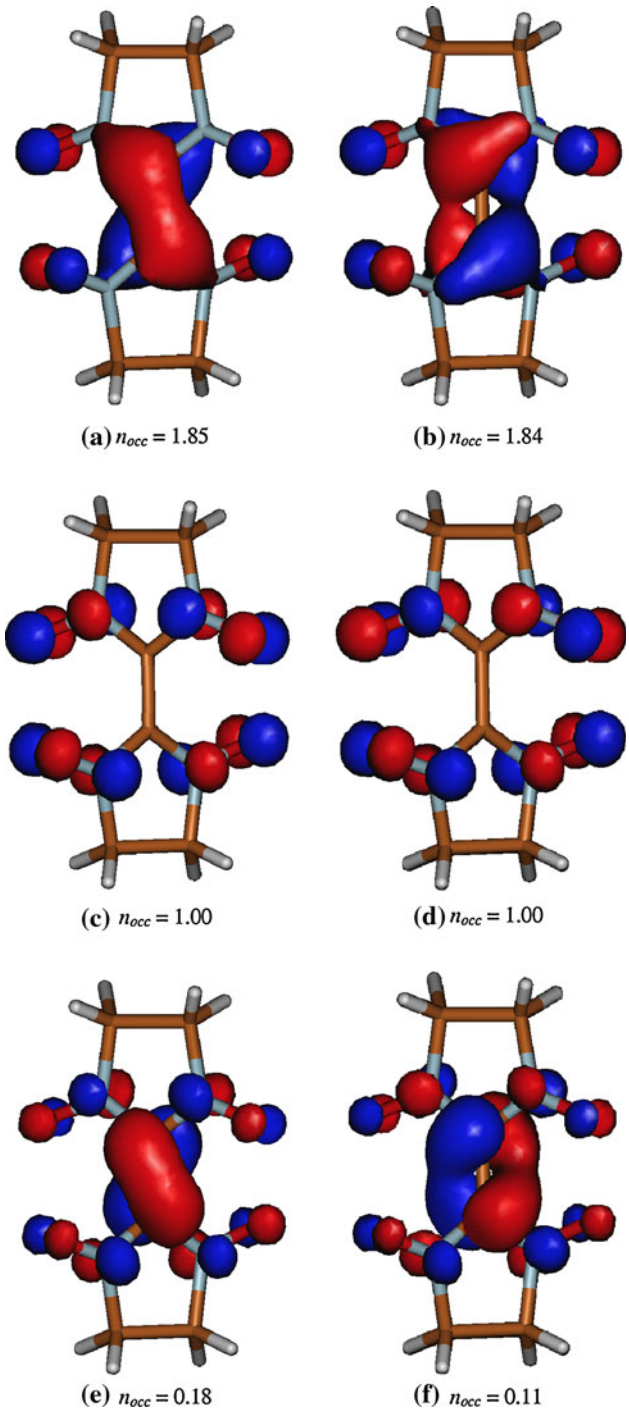

Fig. 4 Active orbitals of the bis(nitronyl) nitroxide biradical. The CAS(2,2) is formed by orbitals **c** and **d**. The listed occupation numbers (n_{occ}) correspond to CAS(6,6)SCF wave function of the triplet state

are underestimated with respect to the experimental ones. However, the DDCI2 description seems to be correct, in agreement with previous evaluations by Castell et al. [86]. The values reported in the previous work are slightly larger than the present ones. This is mainly due to the different

Table 4 Magnetic coupling constant (cm^{-1}) for Ullman's biradicals obtained from different approaches

	Bis(nitronyl) nitroxide		Bis(imino) nitroxide	
	CAS(2,2)	CAS(6,6)	CAS(2,2)	CAS(6,6)
CASSCF	−30	−329	−7	−74
CASPT2	−496	−461	−90	−299
NEVPT2	−510	−332	−66	−212
CAS + S	−254	−319	−93	−104
DDCI2	−265	−275	−99	−94
DDCI	−89	−295	−26	–
Exp [85]	−311		−194	

Minimal (CAS(2,2)) and extended (CAS(6,6)) reference spaces. Triplet state MOs obtained at CASSCF(2,2) or CASSCF(6,6) used in DDCI calculations

N–C–C–N dihedral angles used in the two calculations. It is known that this parameter has a non-negligible influence on the coupling [86].

For bis(imino) nitroxide, even when a direct comparison between DDCI2 and experimental J value is not possible due to the uncertainty on the experimental J value, the results show a non-negligible drop in J when going from DDCI2 to DDCI considering the minimal CAS as reference wave function. Hence, the DDCI2 value seems to be more plausible than DDCI one. Moreover, the inspection of the singlet wave function indicates that the ionic forms have a negligible weight even after including the correlation effects (see Table 5), which is an unexpected feature for antiferromagnetically coupled systems.

Class-partitioned CI calculations have been performed to rationalize why DDCI with a CAS(2,2) reference wave function fails in reproducing the experimental J value in these systems. The main results are collected in Table 6. As in previous systems, the $1h$-$1p$ excitations concentrate the main effect of the CAS + S space (compare the CAS + S and CAS + $1h$-$1p$ J values). In fact, when these excitations are eliminated of the DDCI space (DDCI—$1h$-$1p$ entry in Table 6), the J values go to zero, indicating a central role on the coupling mechanism. Among all the $1h$-$1p$ excitations, the SP determinants have an astonishingly large AF effect,

Table 5 Ionic/neutral configurations ratio on the singlet wave function for Ullman's biradicals obtained from minimal CAS DDCI calculations

	Bis(nitronyl) nitroxide	Bis(imino) nitroxide
CASCI	0.0274	0.0133
CAS + S	0.0230	0.0233
DDCI2	0.0337	0.0285
DDCI	0.0416	0.0254
CASSCF(6,6)	0.0187	0.0155

Table 6 Class-partitioned CI estimates of J (cm^{-1}) for Ullman's biradicals using the CAS(2,2) triplet state MOs and the minimal active space

	Bis(nitronyl) nitroxide	Bis(imino) nitroxide
CASCI	−28	5
CAS + S	−254	−93
DDCI2	−265	−99
DDCI	−89	−26
CAS + $1h$-$1p$	−257	−58
CAS + SP	−584	−72
DDCI − $1h$-$1p$	2	1
CAS + $1h$-$1p$ + $2h$-$1p$	−151	−7
CAS + $1h$-$1p$ + $1h$-$1p$	−151	−24
DDCI2 + $2h$-$1p$	−160	−61
DDCI2 + $1h$-$2p$	−158	−40

specially for bis(nitronyl) nitroxide biradical (CAS + SP entry in Table 6). The $2h$-$1p$ class of excitations introduces a global F effect, as expected for a system with a negligible weight of the ionic forms (compare DDCI2 and DDCI2 + $2h$-$1p$ values). The mechanism leading to this F effect is not completely clear. A possible candidate is the coupling of the neutral forms through the $2h$-$1p$ with the participation of the $1h$ excitations, i.e. the same as previously discussed for the *meta* phenylene-bridged nitroxide radical, corroborated by the F effect obtained from the CAS + $1h$ + $2h$-$1p$ space ($J = -8$ cm^{-1} for bis(nitronyl) nitroxide, -7 cm^{-1} for bis(imino) nitroxide). But the comparison of the CAS + $1h$-$1p$ (-257 cm^{-1} for nitronyl, -58 cm^{-1} for imino) and the CAS + $1h$-$1p$ + $2h$-1p J values (-151 cm^{-1} for nitronyl, -24 cm^{-1} for imino) also suggests an alternative F mechanism, coupling the neutral forms through the $2h$-$1p$ and the $1h$-$1p$ excitations, N ↔ $2h$-$1p$ ↔ $1h$-$1p$ ↔ $2h$-$1p$ ↔ N. Independently of the specific mechanism, the results indicate that the coupling of the $1h$-$1p$ excitations with the $2h$-$1p$ and $1h$-$2p$ excitations attenuates their AF contribution to the J value.

The analysis of the singlet wave function provides some additional insight about the unusual behavior of DDCI. For bis(nitronyl) nitroxide, the out-of-CAS excitation that carries the largest coefficient corresponds to a SP excitation, involving one occupied π and one virtual π^* both centered on the bridging C(sp^2) atoms (Fig. 5, left). The coefficient of this excitation is 0.1271, 0.1671, 0.1268, and 0.0485 at CAS + S, CAS + SP, DDCI2, and DDCI level, respectively. Similar trend, although with smaller coefficients, is observed for a second SP excitation involving also π and π^* orbitals centered on the bridging C(sp^2) atoms (Fig. 5, right). That is, the SP excitations are important at CAS + S and DDCI2 level, but they almost disappear at the DDCI level. This is probably the origin of

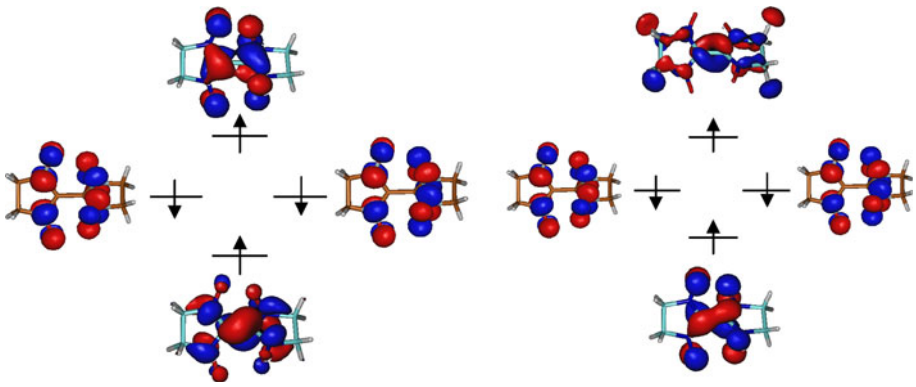

Fig. 5 Dominant SP excitation (*left*) and secondary SP excitation (*right*) for bis(nitronyl) nitroxide system based on a CAS(2,2) reference space

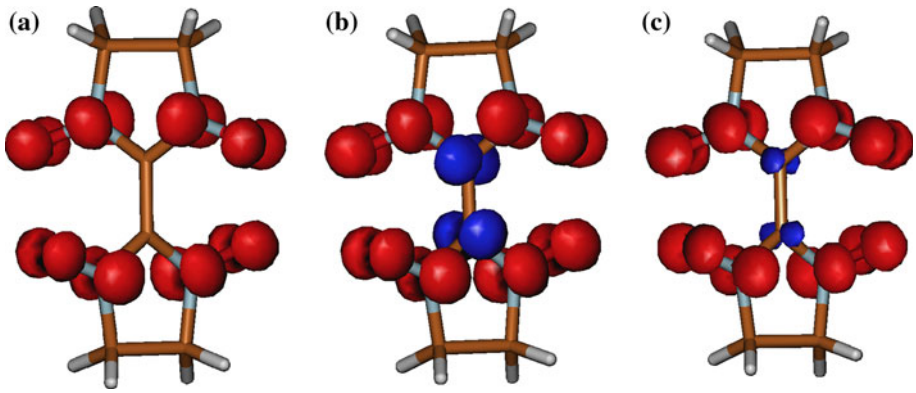

Fig. 6 Triplet spin densities for bis(nitronyl) nitroxide resulting from the **a** CASSCF, **b** CAS + S and **c** DDCI wave function based on a CAS(2,2) active space. The CASSCF, CAS + S and DDCI spin densities based on the CAS(6,6) reference wave function are graphically indistinguishable from (**b**)

the drastic drop in the J value at this level of calculation. The spin population analysis of the CAS + S and DDCI wave functions is in line with the attenuation of the weight of the SP excitations at DDCI level. As can be seen in Fig. 6, the spin population on the bridging C atoms considerably diminishes when going from CAS + S to DDCI. Since it has been found experimentally that the C(sp^2) atom in the nitronyl nitroxide radical has some spin [104–107], it is expected that significant spin density remains in the bis(nitronyl) nitroxide radical. Therefore, the DDCI description based on a minimal (2,2) CAS seems not to be correct.

To take into account the spin polarization on bridging atoms, an alternative strategy consists in enlarging the active space to include those MOs centered on the C(sp^2) atoms. The same strategy has been proposed by Novoa et al. to deal with nitronyl nitroxide radicals [108]. CASSCF(6,6) wave functions are obtained, which include as extra MOs those involved in spin polarization effects. The shape and occupation numbers of these MOs are shown in Fig. 4 and can be compared with those in Fig. 5. The CASSCF(6,6) J value is already in good agreement with the experimental value and the correlation introduces only a minor effect on the coupling constant (Table 4). In fact, spin populations obtained from CASSCF(6,6) and DDCI(6,6) singlet wave functions are practically equivalent (Fig. 6) and close to those obtained at CAS + S(2,2) or DDCI2 (2,2) levels.

It is worth to notice that the CASSCF(6,6) wave function includes all the dominant 1h-1p excitations discussed earlier, in particular the leading SP determinants. That is, once all the neutral forms and (dominant) 1h-1p excitations are correctly described, the singlet–triplet gap is in line with the experimental estimate.

Regarding the bis(imino) nitroxide biradical, the analysis of the singlet wave function gives a similar picture as for bis(nitronyl) nitroxide compound. The dominant out-of-CAS excitation is also a SP excitation, centered on the bridging C(sp2) and the N(imino) atoms. The coefficient of this excitation is 0.0555, 0.0468, 0.0554, and 0.0211 at CAS + S, CAS + SP, DDCI2, and DDCI level, respectively. A secondary SP excitation is also present, with the same nature and behavior. As in the case of bis(nitronyl) nitroxide, there exists a direct relationship between the weight of this excitation and the J value. When the CAS is extended with the MOs participating in the dominant SP excitations, the CASSCF(6,6) J value is already in good agreement with the DDCI(2,2) value. Correlation introduces different effects on the coupling constant (Table 4) depending on the approach. Focusing on the CI results, the correlation produces a small increase in the J value, which at CAS + S(6,6) has practically the same amplitude as at DDCI2(2,2) level. In fact, spin populations obtained from CASSCF(6,6) and DDCI2(6,6) singlet wave functions are practically equivalent and close to those obtained at DDCI2

(2,2) level. This leads to the conclusion that because of the crucial role of the SP excitations included the CAS(6,6), no other significant differential effect is added by out-of CAS electron correlation.

As for the CASPT2 and NEVPT2 results, our comment is based essentially on the bis(nitronyl) nitroxide values, for which the comparison with the experimental data is more grounded. As already said, both the CASPT2 and NEVPT2 values are overestimated with respect to experiment when based on the CAS(2/2) zero-order wave function. The analysis previously reported indicates that this wave function is defective in describing the spin density on the bridging carbon atoms and that this quantity clearly affects the amplitude of *J*. Such a poor description at the zero order is improved at the second-order level, but the correction is excessive in bis(nitronyl) nitroxide (while it looks reasonable in bis(imino) nitroxide). At this level, both second-order theories behave almost in the same way. The enlargement of the active space, introducing the relevant SP excitations, brings about a clear improvement of the zero-order wave function, correctly reproducing the spin density on the bridging C atoms. In this case, NEVPT2 behaves correctly, giving a *J* value in close agreement with the more refined variational approaches. On the contrary, the CASPT2 value (-460 cm^{-1}, close to the one obtained with the CAS(2,2) wave function, -496 cm^{-1}) remains far from the best estimates, indicating the importance of the bielectronic interactions among the active electrons taken into account at the zero order in NEVPT2 and ignored in CASPT2. In bis(imino) nitroxide, the analysis is more difficult, given the difficulty in obtaining reliable reference values.

In summary, the Ullman's compounds present a particular behavior that can be characterized as follows:

1. The DDCI (2,2) *J* values are underestimated with respect to the experimental ones. However, a good agreement is obtained at DDCI2(2,2) level.
2. Spin densities are correct at DDCI2(2,2) level, showing non-negligible contributions on the bridging C atoms, but largely underestimated at DDCI(2,2) level.
3. The singlet wave function is concentrated on the neutral forms at any level, which is an unexpected feature for antiferromagnetic systems.
4. Spin polarization excitations involving the π and π^* MOs centered on the C–C bridge play a crucial role.
5. When these π and π^* MOs are included in the CAS, the *J* value and spin densities are correct at CASSCF level, the out-of-CAS correlation playing a minor (or even negligible) role.

Two possible conclusions can be drawn from these evidences. The first one concerns the adequacy of the DDCI space. As mentioned in Sect. 4, the choice of the determinants to be included in the DDCI space is based on second-order perturbation theory. In fact, the DDCI2 list is obtained from second-order arguments taking the neutral VB forms as degenerate model space. The model space to generate the DDCI list contains both the neutral and ionic VB forms and is in fact no longer degenerated. The extension from DDCI2 to DDCI was originally proposed in the past [109, 110] to deal with systems with large antiferromagnetic coupling, where the ionic VB forms play a crucial role in the kinetic exchange, and hence, present large coefficients on the singlet wave functions. Indeed the DDCI results compare in general very good to experiment [111, 112].

Ullman's compounds, however, seem not to belong to this group since the ionic VB forms have a negligible weight. This suggests that the difference-dedicated CI list constrained to the DDCI2 space contains all the electron correlation contributions playing a differential role in the singlet–triplet gap for these biradicals. The addition of the complementary excitations included in DDCI introduces new effects. The analysis here reported suggests that such effects are unphysical and that they can be reduced (or even removed) by higher order excitations, not included in the DDCI space based on the CAS(2,2) reference wave function. The identification of the nature of these effects and of the mechanisms which cancel them have not been faced here and will be tackled in future works. However, even in absence of such an analysis, a pragmatic approach allows us to suggest to restrict the variational calculations to the DDCI2 space for this kind of systems.

The second idea concerns the adequacy of a minimal (2,2) CAS to deal with these systems. The nitronyl nitroxide radical is a three orbital/three electron system (Scheme 4) [108], where the singly occupied MO has a node on the C(sp2) atom.

In the bis(nitronyl) nitroxide biradical, the two unpaired electrons are placed on the symmetric and antisymmetric combinations of the ϕ_2 SOMO of each unit, which constitute the minimal (2,2) CAS. This CAS contains the two neutral and two ionic VB forms. In most of the transition metal binuclear magnetic systems, this model space is correct and the magnetic coupling constant estimated by DDCI calculations on the basis of this minimal CAS are in good agreement with experimental data. However, for Ullman's compound, the bonding and antibonding MOs resulting from the combination of ϕ_1 and ϕ_3 MOs of each unit play an important role on the description of the low-lying states. In particular, the single excitations moving one electron from $\phi_1(a) \pm \phi_1(b)$ to $\phi_3(a) \pm \phi_3(b)$ (referred above as the π and π^* MOs) have a large weight on the singlet and triplet wave functions. It is important to notice that these 4 MOs and the SOMOs belong to different irreducible representations. Extending the CAS with these

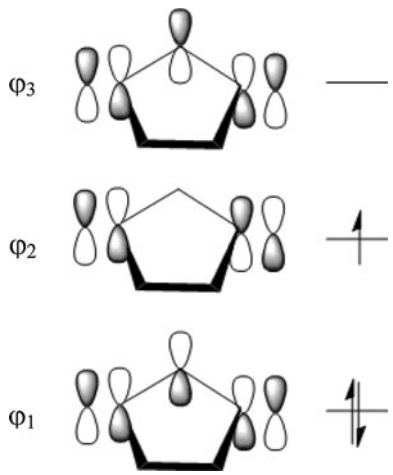

Scheme 4 Three electron/three orbital description of the nitronyl nitroxide radical

four additional MOs ensure a correct description of these excitations, and consequently of the J value and the spin densities on the bridging C atoms.

Since the out-of-CAS correlation acting on these CASSCF(6,6) wave functions does not introduce important additional effects (neither in J, nor in the spin population), the main effect is already present at this level, in particular, the leading $1h$-$1p$ excitations involving the $\phi_1(a) \pm \phi_1(b)$ and $\phi_3(a) \pm \phi_3(b)$ MOs. This is probably the key to understand the equivalence between CASSCF(6,6) and DDCI2(2,2) results.

6 Conclusions

The magnetic coupling constants in a set of nitroxide organic biradicals have been calculated with different ab initio wave function-based methods and the magnetic pathways analyzed from class-partitioned CI calculations. The leading mechanisms governing the coupling have been isolated and compared to those previously reported for dinuclear metallic magnetic compounds.

We have focused on two well-studied examples: phenylene-bridged nitroxide biradicals and Ullman's bis(nitronyl) and bis(imino) nitroxides. *Para* phenylene-bridged nitroxide biradical and Ullman's compounds are all antiferromagnetically coupled systems, with large coupling constant in the case of *para* phenylene biradical and moderate constants in the case of Ullman's compounds, while *meta* phenylene-bridged nitroxide is ferromagnetic. The nature of the interaction has been successfully predicted by all the considered methods, the amplitude being in general best reproduced by the DDCI approach. Regarding the leading mechanisms, both *para* and *meta* phenylene-bridged nitroxide biradicals essentially behave in a similar way as binuclear transition metal magnetic systems. An additional mechanism involving $1h$-$1p$ and $2h$-$1p$ excitations seems to play a non-negligible role in these systems. This mechanism has not been previously isolated in metallic biradicals, probably because the π framework in conjugated biradical systems provides a set of occupied and virtual MOs close in energy to the orbitals of the CAS, and hence, the corresponding $1h$-$1p$ excitations are of lower energy than in TM compounds, resulting in a larger impact on the magnetic coupling amplitude.

Regarding Ullman's compounds, it has been found that DDCI calculations based on a minimal (2,2) CAS fail in reproducing both the J value and the spin density populations. The $1h$-$1p$ excitations play a crucial role, in particular those introducing spin polarization effects on the bridging atoms, with large coefficients in singlet and triplet wave functions. To take into account the SP effects, the CAS is extended with two π occupied and two π^* virtual MOs involving the bridging atoms. The J values obtained with this (6,6) CAS are in good agreement with experimental data, and there is a considerable spin density on the C(sp2) atom even without introducing additional dynamical correlation, which indicates that the main effects are already present at CASSCF level.

These results suggest some final remarks. Transition metal magnetic complexes differ from organic biradicals in several aspects:

1. The relative position of the magnetic orbitals with respect to the rest of occupied and virtual MOs. Small energetic gaps are expected among the active orbitals and the valence MOs, in particular in conjugated π systems, while in general this is not the case for TM complexes. This has an important consequence on the energy associated to the intermediate states involved in the different pathways governing the coupling between the active sites. The smaller the excitation energy of the intermediate, the larger its contribution to the coupling. This can introduce additional mechanisms, not found previously in TM magnetic systems, change the leading mechanism, or even the relative contributions to J of competing mechanisms.
2. The delocalization of the active orbitals. In TM complexes, active orbitals are essentially centered on the metal atoms, with delocalization tails on the nearest neighbors. However, active orbitals in organic biradicals are not constrained to a reduced portion of the molecule, but in general they present contributions of several atoms in the system. This implicit delocalization of the active electrons makes difficult to distinguish between active and bridging centers, and it can require, as in the case of Ullman's compounds, extra MOs to correctly describe the active part of the

system. Geometrical parameters often used in magneto-structural correlations such as the mean distance between active centers R_{ab} or the bond angles lose their meaning. Indeed, parameters such as the on-site Coulomb repulsion, U, or the hopping integral, t_{ab} take very different values than those reported for TM complexes. Hence, models such as Anderson model conceived for localized spin could fail in describing these systems.

For these reasons, the rationalization of the mechanisms governing the magnetic coupling in pure organic systems based on the analysis previously established for TM complexes could be neither adequate nor complete. Instead, it would require a (partial) reformulation of the leading physical mechanisms as well as theoretical procedures adapted to deal with the special features of these systems.

Acknowledgments Financial support has been provided by the Spanish Ministerio de Ciencia e Innovación (Projects CTQ2009-07767 and CTQ2008-06644-C02-01) and the Generalitat de Catalunya (Project 2009SGR462 and Xarxa d'R + D+I en Quîmica Teòrica i Computacional, XRQTC).

References

1. Anderson PW (1950) Phys Rev 79:350
2. Anderson PW (1963) In: Turnbull F, Seitz F (eds) Theory of the Magnetic Interaction: exchange in insulators and superconductors, Solid State Physics, vol 14. Academic Press, New York, p 99
3. For a recent revision, see: Van den Heuvel W, Chibotaru LF (2007) Phys Rev B 76:104424
4. Malrieu JP, Guihery N, Calzado CJ, Angeli C (2007) J Comp Chem 28:35
5. Illas F, de Moreira PR I, de Graaf C, Barone V (2000) Theoret Chem Acc 104:265
6. Adamo C, Barone V, Bencini A, Broer R, Filatov M, Harrison NM, Illas F, Malrieu JP, Moreira I de PR (2006) J Chem Phys 124:107101
7. Ruiz E, Cano J, Alvarez S, Polo V (2006) J Chem Phys 124:107102
8. Bencini A (2008) Inorg Chim Acta 361:3820
9. de Moreira PR I, Illas F (2006) Phys Chem Chem Phys 8:1645
10. de Loth P, Cassoux P, Daudey JP, Malrieu JP (1981) J Am Chem Soc 103:4007
11. Charlot MF, Verdaguer M, Journaux Y, de Loth P, Daudey JP (1984) Inorg Chem 23:3802
12. Daudey JP, de Loth P, Malrieu JP (1985) In: Willett RD, Gatteschi D, Kahn O (eds) Magneto-Structural Correlation in exchange coupled systems, NATO Advanced Studies Series. C, vol 140. Reidel, Dordrecht, p 87
13. Malrieu JP (1967) J Chem Phys 47:4555
14. Broer R, Maaskant WJA (1986) Chem Phys 102:103
15. Miralles J, Daudey JP, Caballol R (1992) Chem Phys Lett 198:555
16. Miralles J, Castell O, Caballol R, Malrieu JP (1993) Chem Phys 172:33
17. Neese F (2003) J Chem Phys 119:9428
18. Neese F, Petrenko T, Ganyushin D, Olbrich G (2007) Coord Chem Rev 251:288
19. Barone V, Cacelli I, Ferretti A, Girlanda M (2008) J Chem Phys 128:174303
20. Castell O, Caballol R, García VM, Handrick K (1996) Inorg Chem 35:1609
21. Cabrero J, Ben Amor N, de Graaf C, Illas F, Caballol R (2000) J Phys Chem A 104:9983
22. Suaud N, Gaita-Arino A, Clemente-Juan JM, Sánchez-Marín J, Coronado E (2002) J Am Chem Soc 124:15134
23. Herebian D, Wieghart KE, Neese F (2003) J Am Chem Soc 125:10997
24. Cabrero J, de Graaf C, Bordas E, Caballol R, Malrieu JP (2003) Chem Eur J 9:2307
25. Neese F (2006) J Am Chem Soc 128:10213
26. Calzado CJ, Evangelisti S, Maynau D (2003) J Phys Chem A 107:7581
27. Aronica C, Jeanneau E, El Moll H, Luneau D, Gillon B, Goujon A, Cousson A, Carvajal MA, Robert V (2007) Chem Eur J 13:3666
28. Bonnet ML, Aronica C, Chastanet G, Pilet G, Luneau D, Mathoniere C, Clerac R, Robert V (2008) Inorg Chem 47:1127
29. Neese F (2004) Magn Reson Chem 43:S187
30. McNaughton RL, Roemelt M, Chin JM, Schrock RR, Neese F, Hoffman BM (2010) J Am Chem Soc 132:8645
31. Rota JB, Norel L, Train C, Ben Amor N, Maynau D, Robert V (2008) J Am Chem Soc 130:10380
32. Queralt N, Taratiel D, de Graaf C, Caballol R, Cimiraglia R, Angeli C (2008) J Comp Chem 29:994
33. Vancoillie S, Chalupsky J, Ryde U, Solomon EI, Pierloot K, Neese F, Rulisek L (2010) J Phys Chem B 114:7692
34. de Graaf C, Hozoi L, Broer R (2004) J Chem Phys 120:961
35. Casanovas J, Rubio J, Illas F (1996) Phys Rev B 53:945
36. Calzado CJ, Sanz JF, Malrieu JP (2000) J Chem Phys 112:5158
37. de Graaf C, Sousa C, Moreira I de PR, Illas F (2001) J Phys Chem A 105:11371
38. Suaud N, Lepetit MB (2002) Phys Rev Lett 88:56405
39. Calzado CJ, de Graaf C, Bordas E, Caballol R, Malrieu JP (2003) Phys Rev B 67:132409
40. Noodleman L, Davidson ER (1986) Chem Phys 109:131
41. Noodleman L, Case DA (1992) Adv Inorg Chem 38:423
42. Yamaguchi K (1975) Chem Phys Lett 30:288
43. Soda T, Kitagawa Y, Onishi T, Takano Y, Shigeta Y, Nagao N, Yoshioka Y, Yamaguchi K (2000) Chem Phys 319:223
44. Caballol R, Castell O, Illas F, Moreira I de PR, Malrieu JP (1997) J Phys Chem A 101:7860
45. Ruiz E, Cano J, Alvarez S, Alemany P (1999) J Comput Chem 20:1391
46. Ruiz E, Alvarez S, Cano J, Polo V (2005) J Chem Phys 123:164110
47. Illas F, de Moreira PR I, Bofill JM, Filatov M (2006) Theor Chem Acc 116:587
48. Rudra I, Wu Q, Van Voorhis T (2006) J Chem Phys 124:024103
49. Filatov M, Shaik S (2000) J Phys Chem A 104:6628
50. Bencini A, Totti F, Daul CA, Doclo K, Fantucci P, Barone V (1997) Inorg Chem 36:5022
51. Daul CA (1994) Int J Quant Chem 52:867
52. Atanasov M, Daul CA, Rauzy C (2003) Chem Phys Lett 367:737
53. Atanasov M, Daul CA (2003) Chem Phys Lett 379:209
54. Ruiz E, Alemany P, Alvarez S, Cano J (1997) J Am Chem Soc 119:1297
55. Ruiz E, Cano J, Alvarez S, Alemany P (1998) J Am Chem Soc 120:11122
56. Alvarez S, Ruiz E (2010) Chem Eur J 16:2726
57. Martin RL, Illas F (1997) Phys Rev Lett 79:1539

58. Franchini C, Bayer V, Podloucky R, Paier J, Kresse G (2005) Phys Rev B 72:045132
59. Valero R, Costa R, Morerira I de PR, Truhlar DG, Illas F (2008) J Chem Phys 128:114103
60. Zein S, Kalhor MP, Chibotaru LF, Chermette H (2009) J Chem Phys 131:224316
61. Rivero P, Moreira I de PR, Scuseria GE, Illas F (2009) Phys Rev B 79:245129
62. Comba P, Hausberg S, Martin B (2009) J Phys Chem A 113:6751
63. Ciofini I, Illas F, Adamo C (2004) J Chem Phys 120:3811
64. Feng X, Harrison NM (2004) Phys Rev B 70:092402
65. Cramer CJ, Truhlar DG (2009) Phys Chem Chem Phys 11:10757
66. Neese F (2009) Coord Chem Rev 253:526
67. Calzado CJ, Cabrero J, Malrieu JP, Caballol R (2002) J Chem Phys 116:2728
68. Calzado CJ, Angeli C, Taratiel D, Caballol R, Malrieu JP (2009) J Chem Phys 131:044327
69. Heisenberg W (1928) Z Phys 49:619
70. Dirac PAM (1947) The principles of quantum mechanics. Clarendon, Oxford
71. Van Vleck JH (1932) The theory of electric and magnetic susceptibilities. Oxford University Press, Oxford
72. Brillouin L (1932) J Phys (Paris) 3:373
73. Generalized theorem: Levy B, Berthier G (1968) Int J Quant Chem 2:307
74. Ullman EF, Boocock DGB (1969) J Chem Soc D:1161
75. Dvolaitzky M, Chiarelli R, Rassat A (1992) Angew Chem Int Ed Engl 31:180
76. Kanno F, Inoue K, Koga N, Iwamura H (1993) J Am Chem Soc 115:847
77. Fang S, Lee MS, Hrovat DA, Borden WT (1995) J Am Chem Soc 117:6727
78. Trindle C, Datta SN (1996) Int J Quant Chem 57:781
79. Mitani M, Yamaki D, Takano Y, Kitagawa Y, Yoshioka Y, Yamaguchi K (2007) J Chem Phys 113:2000
80. Catala L, Le Moigne J, Kyritsakas N, Rey P, Novoa JJ, Turek P (2001) Chem Eur J 7:2466
81. Barone V, Cacelli I, Cimino P, Ferreti A, Monti S, Prampolini G (2009) J Phys Chem A 113:15150
82. Barone V, Cacelli I, Ferretti A (2009) J Chem Phys 130:094306
83. Barone V, Cacelli I, Ferretti A, Prampolini G (2009) J Chem Phys 131:224103
84. Ishida T, Iwamura H (1991) J Am Chem Soc 113:4238
85. Alies F, Luneau D, Laugier J, Rey P (1993) J Phys Chem 97:2922
86. Castell O, Caballol R, Subra R, Grand A (1995) J Phys Chem 99:154
87. Ali ME, Datta SN (2006) J Phys Chem A 110:2776
88. Barone V, Bencini A, di Matteo A (1997) J Am Chem Soc 119:10831
89. Andersson K, Malmqvist PÅ, Roos BO, Sadlej AJ, Wolinski K (1990) J Phys Chem 94:5483
90. Andersson K, Roos BO (1992) Chem Phys Lett 191:507
91. Andersson K, Malmqvist PÅ, Roos BO (1992) J Chem Phys 96:1218
92. Angeli C, Cimiraglia R, Evangelisti S, Leininger T, Malrieu JP (2001) J Chem Phys 114:10252
93. Angeli C, Cimiraglia R, Malrieu JP (2001) Chem Phys Lett 350:297
94. Angeli C, Cimiraglia R, Malrieu JP (2002) J Chem Phys 117:9138
95. Angeli C, Pastore M, Cimiraglia R (2007) Theor Chem Acc 117:743
96. Dyall KG (1995) J Chem Phys 102:4909
97. Roos BO, Lindh R, Malmqvist PÅ, Veryazov V, Widmark PO (2004) J Phys Chem A 108:2851
98. Ghigo G, Roos BO, Malmqvist PÅ (2004) Chem Phys Lett 396:142
99. Aquilante F, De Vico L, Ferré N, Ghigo G, Malmqvist PÅ, Neogrady P, Pedersen TB, Pitonák M, Reiher M, Roos BO, Serrano-Andrés L, Urban M, Veryazov V, Lindh R (2010) J Comput Chem 31:224
100. Ben Amor N, Maynau D (1998) Chem Phys Lett 286:211
101. Ovchinnikov AA (1978) Theor Chim Acta 10:297
102. Yamaguchi K, Fueno T (1989) Chem Phys Lett 159:465
103. Yamaguchi K, Okumura M, Nakano M (1992) Chem Phys Lett 191:237
104. Zheludev A, Barone V, Bonnet M, Delley B, Grand A, Ressouche E, Subra R, Schweizer J (1994) J Am Chem Soc 116:2019
105. Romero FM, Ziessel R, Bonnet M, Pontillon Y, Ressouche E, Schweizer J, Delley B, Grand A, Paulsen C (2000) J Am Chem Soc 122:1298
106. Barone V, Grand A, Luneau D, Rey P, Minichino C, Subra R (1993) New J Chem 17:545
107. Barone V, Bencini A, Cossi M, di Matero A, Mattesini M, Totti F (1998) J Am Chem Soc 120:7069
108. Novoa JJ, Lafuente P, Deumal M, Mota F (2002) In: Miller JS, Drillon M (eds) Magnetism: molecules to materials, vol. 4. Wiley, New York, p 65
109. Calzado CJ, Sanz JF, Malrieu JP (2000) J Chem Phys 112:5158
110. Calzado CJ (1998) PhD Thesis, Universidad de Sevilla
111. de Moreira PR I, Illas F, Calzado CJ, Sanz JF, Malrieu JP, Ben Amor N, Maynau D (1999) Phys Rev B 59:6593
112. Muñoz D, Illas F, Moreira I de PR (2000) Phys Rev Lett 84:1579